

## Resonant vibration of piezoceramic plates in fluid

Yu-Chih Lin\*

*Department of Biomedical Engineering, Yuanpei University, Hsinchu, Taiwan 300, Republic of China*

Chien-Ching Ma<sup>‡</sup>

*Department of Mechanical Engineering, National Taiwan University, Taipei, Taiwan 106, Republic of China*

*(Received December 3, 2007, Accepted May 12, 2008)*

**Abstract.** In this paper, both experimental measurement and theoretical analysis are used to investigate the out-of-plane resonant characteristics of a cantilevered piezoceramic plate in air and three different kinds of fluid. The experimental method, amplitude-fluctuation electronic speckle pattern interferometry (AF-ESPI), is the major technique used in this study to measure the resonant characteristics of the cantilevered piezoceramic plate. Both resonant frequencies and full-field mode shapes are obtained from this experimental technique. Numerical computations based on the finite element analysis are presented for comparison with the experimental results. Good quality of mode shapes for the cantilevered piezoceramic plate in air is obtained from the AF-ESPI technique. However, the quality decreases as the viscosity of fluids increases. From the results provided from experimental measurements and numerical computations, it is indicated that the resonant frequencies of the cantilevered piezoceramic plate in fluid decrease with the increase of the viscosity of fluids. Good agreements between the experimental measured data and the numerical calculated results are found for both resonant frequencies and mode shapes of the cantilevered piezoceramic plate in fluid.

**Keywords:** piezoceramic plate; fluid; electronic speckle pattern interferometry; resonant frequencies; mode shape.

---

### 1. Introduction

The piezoelectric effect is applied to many modern engineering applications because it expresses the connection between the electrical and mechanical fields. The piezoelectric materials can generate driving forces as the actuators upon the application of the electric field due to the inverse piezoelectric effect. Conversely, they can be used as sensors due to the direct piezoelectric effect. The piezoelectric materials are widely used in many fields such as the electromechanical transducers, underwater acoustics, resonators, ultrasonics, and MEMS. Since acoustic wave is the only one that can transmit energy underwater for a long distance, the ultrasonic transducers are widely used in navigation, petroleum acoustics, underwater communication, military, and investigation of creatures in the sea. Hence, the study of the vibration characteristics of piezoelectric devices in fluid has received considerable attention in recent years.

---

\* Assistant Professor, E-mail: [d87522011@ntu.edu.tw](mailto:d87522011@ntu.edu.tw)

<sup>‡</sup> Professor, Corresponding author, E-mail: [ccma@ntu.edu.tw](mailto:ccma@ntu.edu.tw)

Numerical methods have been widely used to analyze the characteristics of piezoelectric materials in fluid. Ekeom *et al.* (1998) used a numerical model to present in the frequency domain the radiation of a piezoelectric transducer in a fluid-filled borehole surrounded by an infinite extent. Balabaev and Ivina (2001) used the combined finite-element-boundary method to solve the problem on the radiation of a water-filled piezoceramic cylinder. The frequency characteristics of the transmitting response of the piezoelectric cylinder were obtained along with the frequency characteristics of the acoustic power, the directional characteristics, the velocity and pressure distributions over the radiating cylindrical surfaces. A transport model for high-frequency vibration power flows in coupled heterogeneous structures was proposed by Savin (2008) which can be used in subsequent computations to solve numerically the transport equations for coupled systems.

Because of the technical difficulties, very few results were provided by the experimental methods for the vibration characteristics of piezoelectric materials in fluid, especially for the full-field measurement. Oswin *et al.* (1994) and Petzing *et al.* (1996) employed the electronic speckle pattern interferometry (ESPI) and electronic speckle pattern shearing interferometry (ESPSI) techniques, respectively, to investigate the flexensional transducer vibration patterns underwater. They found that it was more difficult to obtain the experimental results in-fluid than in-air using ESPI technique. The quality of experimental results obtained by Oswin *et al.* (1994) was poor. Petzing *et al.* (1996) found that the ESPSI technique can improve the quality of image in fluid. The experimental data indicated that the resonant frequency decreased when the transducers were operated in water and that the resonant mode shapes were slightly different from that in-air. Although the image fringe obtained from the experiment is sufficient to allow potentially further computer-based post-processing of the data, some efforts on improving the image quality and the experimental techniques are still needed. The objective of this paper is to investigate the out-of-plane resonant frequencies and correspondent full-field mode shapes of a cantilevered piezoceramic plate in various fluids using both theoretical and experimental techniques.

The electronic speckle pattern interferometry (ESPI) experimental technique can provide the full-field deformation of the vibrating piezoceramic plate in resonance. It was first proposed by Butters and Leendertz (1971) and was improved by numerous researchers (e.g. Nakadate *et al.* 1986, Jones and Wykes 1989, Shellabear and Typer 1991, Graham *et al.* 1999) to become an advanced technique for vibration analysis. The most convenient experimental setup of vibration measurement by ESPI is the time-averaging method that yields a video image of vibrating object with correlation fringes superimposed. However, the restrictions of the time-averaging method are decreased visibility with vibration amplitude, and limited numbers of fringes. Wang *et al.* (1996) proposed the amplitude-fluctuation ESPI (AF-ESPI) technique based on video-signal-subtraction, but the reference image was taken from a vibrating state instead of a free state. The fringe patterns obtained by AF-ESPI method have enhanced visibility and reduced noise. Huang and Ma (1998) and Ma and Huang (2001) further applied the amplitude-fluctuation ESPI (AF-ESPI) to investigate three-dimensional volume vibrations of piezoelectric materials. In their works, the interferometric fringe patterns obtained by AF-ESPI were clearly displayed with high quality for identification of resonant frequencies and mode shapes.

In this paper, both experimental measurement and theoretical analysis are used to investigate the out-of-plane resonant characteristics of a cantilevered piezoceramic plate in air and three different kinds of fluid. Numerical computations based on the finite element method (FEM) utilizing the commercial software package, ABAQUS, is employed to analyze the resonant characteristics of a cantilevered piezoceramic plate in air and fluid. The shell element model is used for in-air analysis.

For the in-fluid analysis, the acoustic analysis is used to obtain the frequencies and the mode shapes of the cantilevered piezoceramic plate. The resonant frequencies measured by AF-ESPI are compared with those computed by FEM. The corresponding mode shapes obtained by AF-ESPI and calculated by FEM are also presented for comparison. It is found in this study that although the difficulties of AF-ESPI experimental measurement increase and the clarity of the mode shape fringes decrease when the density and the viscosity of the fluid increase, the results measured by experiments and FEM are in good agreement. Hence the experimental technique used in this study can be used to measure the resonant characteristic of the piezoceramic plate both in air and in fluid. The full-field mode shapes obtained at resonant frequencies by using the AF-ESPI method, together with the results of the finite element calculation provide complete information of the vibration characteristics of piezoceramic plates in air and in fluid.

## 2. Theory of AF-ESPI technique

The experimental setup and theory of AF-ESPI for out-of-plane vibration measurement were described in detail by Ma and Huang (2001). The experimental setup of AF-ESPI for out-of-plane measurement is shown in Fig. 1. At a given instant time  $t$ , the light intensity in the image plane detected by a charge-coupled device (CCD) camera (Pulnix TM-7CN, Pulnix America, Inc., Sunnyvale, CA) can be expressed as

$$I(t) = I_R + I_O + 2\sqrt{I_R I_O} \cos \left[ \phi + \frac{2\pi}{\lambda} (1 + \cos \theta) A(t) \right] \quad (1)$$

where  $I_R$  is the reference light intensity,  $I_O$  is the object light intensity,  $\phi$  is the phase difference between reference and object light,  $\lambda$  is the wavelength of laser,  $\theta$  is the angle between object light and observation direction, and  $A(t)$  is the vibration amplitude of a given point on the object. The light intensity averaged over the CCD refreshing time  $\tau$  by using the time-averaged method is

$$I_\tau = I_R + I_O + \frac{2\sqrt{I_R I_O}}{\tau} \int_0^\tau \cos \left[ \phi + \frac{2\pi}{\lambda} (1 + \cos \theta) A(t) \right] dt \quad (2)$$

Assuming that the specimen vibrates periodically, the intensity average  $I_\tau$  can be written as

$$\begin{aligned} I_\tau &= I_R + I_O + \frac{2\sqrt{I_R I_O}}{\tau} \int_0^\tau \cos(\phi + \Gamma A \cos \omega t) dt \\ &= I_R + I_O + \frac{2\sqrt{I_R I_O}}{\tau} \operatorname{Re} \left\{ e^{i\phi} \int_0^\tau \exp(i\Gamma A \cos \omega t) dt \right\} \end{aligned}$$

where  $\operatorname{Re}$  stands for the real part,  $A(t) = A \cos \omega t$  and  $\omega$  is the angular frequency.  $\Gamma = \frac{2\pi}{\lambda} (1 + \cos \theta)$  and  $\tau = \frac{2m\pi}{\omega}$ , where  $m$  is an integer. The intensity of the first image, named as the reference image, can be expressed as

$$I_\tau = I_R + I_O + 2\sqrt{I_R I_O} |(\cos \phi) J_0(\Gamma A)| \quad (3)$$

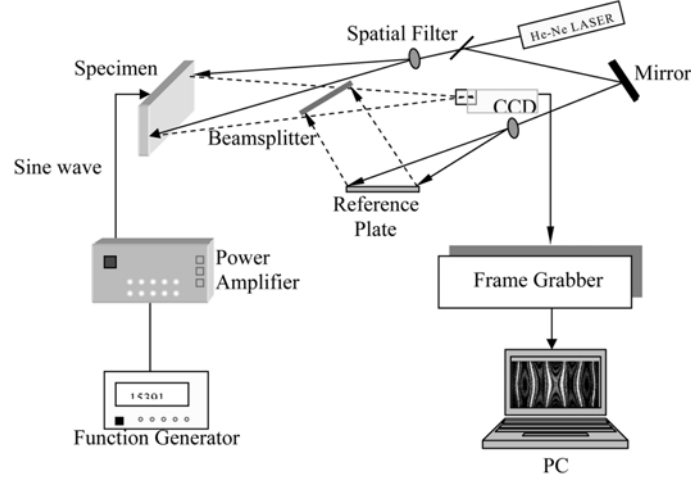


Fig. 1 Schematic diagram of the AF-ESPI setup for out-of-plane measurement

where  $J_0$  is a zeroth order Bessel function of the first kind. As the vibration of the specimen continues, we can assume that the vibration amplitude changes from  $A$  to  $A + \Delta A$  because of the electronic noise or instability of the apparatus, then the light intensity of the second image  $I'_\tau$  can be represented as

$$I'_\tau = I_R + I_O + 2\sqrt{I_R I_O} \left| (\cos \phi) \left[ 1 - \frac{1}{4} \Gamma^2 (\Delta A)^2 \right] J_0(\Gamma A) \right| \quad (4)$$

When these two images (the reference and second images) are subtracted by the image processing system, i.e., when Eq. (3) is subtracted from Eq. (4), and are rectified, the resulting image intensity can be expressed as

$$I = I'_\tau - I_\tau = \frac{\sqrt{I_R I_O}}{2} \left| (\cos \phi) \Gamma^2 (\Delta A)^2 J_0(\Gamma A) \right| \quad (5)$$

### 3. Specimens and experimental set-up

The dimension of the specimen is  $65 \text{ mm} \times 25 \text{ mm} \times 0.26 \text{ mm}$  as shown in Fig. 2. The thin piezoceramic plate is made of  $Pb(Zr, Ti)O_3$  ceramics with the model number PIC-151 (Physik Instrumente). The material properties of this thin piezoceramic plate are listed in Table 1. Two opposite faces of this piezoceramic plate are completely coated with silver electrodes. The fixed-end boundary condition is applied to the short edge of the specimen, and the other three edges are set to be free. The cantilevered piezoceramic plate is excited by the application of a time harmonic voltage across electrodes on two surfaces of this plate. When the frequency of excitation is near the resonant frequencies of the cantilevered piezoceramic plate, this specimen is in resonance and the vibration with large displacements is invoked. The specimen is put in the middle of a vessel with the dimension  $80 \text{ mm} \times 80 \text{ mm} \times 80 \text{ mm}$ . This vessel is not so large because of the visibility and feasibility for the optical experimental measurement. In order to increase the intensity of light

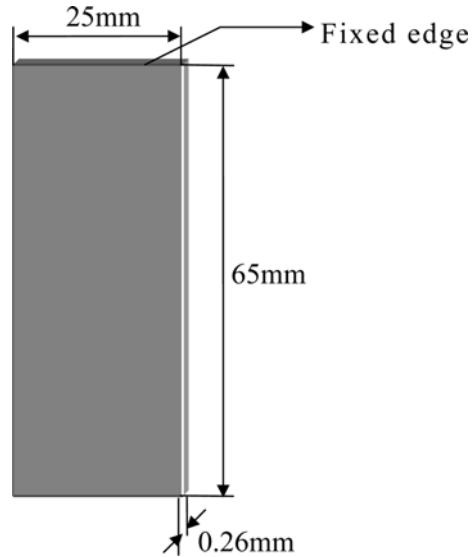


Fig. 2 Schematic diagram of the geometric dimensions and boundary conditions of the piezoceramic plate

Table 1 Material properties of PIC-151

QUALITY	PIC-151
$C_{11}^E$ (N/m <sup>2</sup> )	$10.76 \times 10^{10}$
$C_{12}^E$	$6.313 \times 10^{10}$
$C_{13}^E$	$6.386 \times 10^{10}$
$C_{33}^E$	$10.04 \times 10^{10}$
$C_{44}^E$	$1.962 \times 10^{10}$
$C_{66}^E$	$2.224 \times 10^{10}$
$e_{31}$ (N/Vm)	-9.52
$e_{33}$	15.14
$e_{15}$	11.97
$\rho$ (Kg/m <sup>3</sup> )	7800
$\epsilon_{11}^s / \epsilon_0$	1111
$\epsilon_{33}^s / \epsilon_0$	925
$\epsilon_0$	$8.85 \times 10^{-12}$

reflection from the specimens and the contrast of fringe patterns, the surfaces of the piezoceramic plate are coated with white paint, which is mixed with fine seaweed powder. Table 2 lists the material properties of the fluid which include air, water, glycerine, and fructose.

The optical layout of the self-arranged AF-ESPI systems, as shown in Fig. 1, is used to perform the out-of-plane measurements for resonant frequencies and corresponding mode shapes. A He-Ne

Table 2 Material constants of fluids

Material Constants	Fluids			
	Air	Water	Glycerine	Fructose
Bulk Modulus (N/m <sup>2</sup> )	$1.42 \times 10^5$	$2.2 \times 10^9$	$4.39 \times 10^9$	$8.43 \times 10^9$
Density (Kg/m <sup>3</sup> )	1.2	1000	1260	1570
Wave Velocity (m/s)	344	1483	1875	2317
Viscosity (Pa · s)	0.00001	0.001	1.2	2.5

laser (Melles Griot 05-LHP-928) with 35 mW and wavelength  $\lambda = 632.8$  nm is used as the coherent light source. The emitting laser beam is split into two parts by a variable beamsplitter. One beam acting as the object beam is directed toward the piezoceramic plate and then reflected to the CCD camera; the other one which serves as a reference beam is illuminated on the surface of a reference plate and reflected into the CCD camera via the beamsplitter. The object and reference beams are combined into the CCD sensor array through a zoom lens (Nikon Micro-Nikkor 55mm, Nikon, Melville, NY). A CCD camera (Pulnix TM-7CN) and a frame grabber (Dipix P360F) with a digital signal processor on board are used to record and process the images obtained from interferogram of the object and reference beams. Once the specimen vibrates, the interferogram recorded by the CCD camera is stored in an image buffer as a reference image. Then the next frame is grabbed and subtracted by the image processing system. The CCD camera converts the intensity distribution of the interference pattern of the object into a corresponding video signal at 30 frames per second. This signal is electronically processed and finally converted into an image on the video monitor. The interpretation of the fringe image is similar to the reading of a displacement contour. To achieve a sinusoidal output, a digitally controlled function generator (Hewlett Packard, HP-33120A) connected to a power amplifier (NF Electronic Instruments 4005 type) is employed as an input source, which generates periodical exciting force to the specimen.

Detailed experimental procedure of the AF-ESPI technique for the out-of-plane vibration measurement is described as follows. First, a reference image is taken after the specimen vibrates with the second image taken subsequently; the reference image is subtracted by the image processing system. If the vibrating frequency is not the resonant frequency, only randomly distributed speckles are displayed and no fringe patterns will be shown. In case that the vibrating frequency falls in the neighborhood of the resonant frequency, distinct stationary fringe patterns will be observed in the monitor. Then, the function generator is carefully and gradually turned; the number of fringes will increase and the fringe pattern will become clearer as the resonant frequency is approached. From the aforementioned experimental procedure, the resonant frequencies and the correspondent mode shapes can be determined at the same time by using the AF-ESPI optical system. The results are indicated in Fig. 3 and Table 3.

#### 4. Experimental and numerical results

The resonant frequencies and mode shapes of the cantilevered piezoceramic plate in air and in fluid are presented in this section. In addition to the experimental measurements, numerical computations of resonant frequencies and mode shapes are also performed using ABAQUS finite element package, in which the plane shell element model is used. In this study, we analyze the

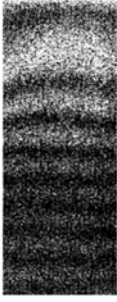
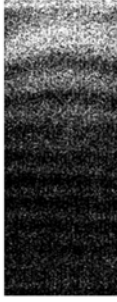
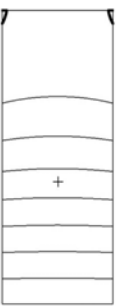
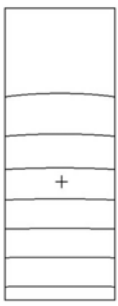
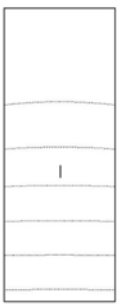
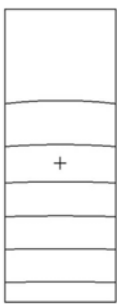
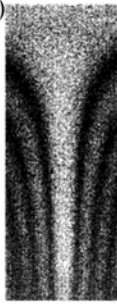
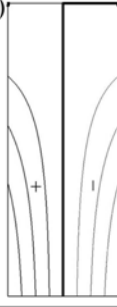
		MODE SHAPE—PIC151			
Mode Number		In air	In water	In Glycerine	In Fructose
<b>1</b> ESPI		(30) 	(10) 	(8) 	(7) 
	FEM	(28) 	(10) 	(9) 	(9) 
<b>2</b> ESPI		(142) 	.....	.....	.....
	FEM	(150) 	(77) 	(71) 	(65) 

Fig. 3 Out-of-plane mode shapes and resonant frequencies of a cantilevered piezoceramic plate in air and fluid obtained by AF-ESPI and FEM

resonant characteristics of the coupled structure-fluid system in steady state. The resonant frequencies and the mode shapes of the cantilevered piezoceramic plate are extracted from the

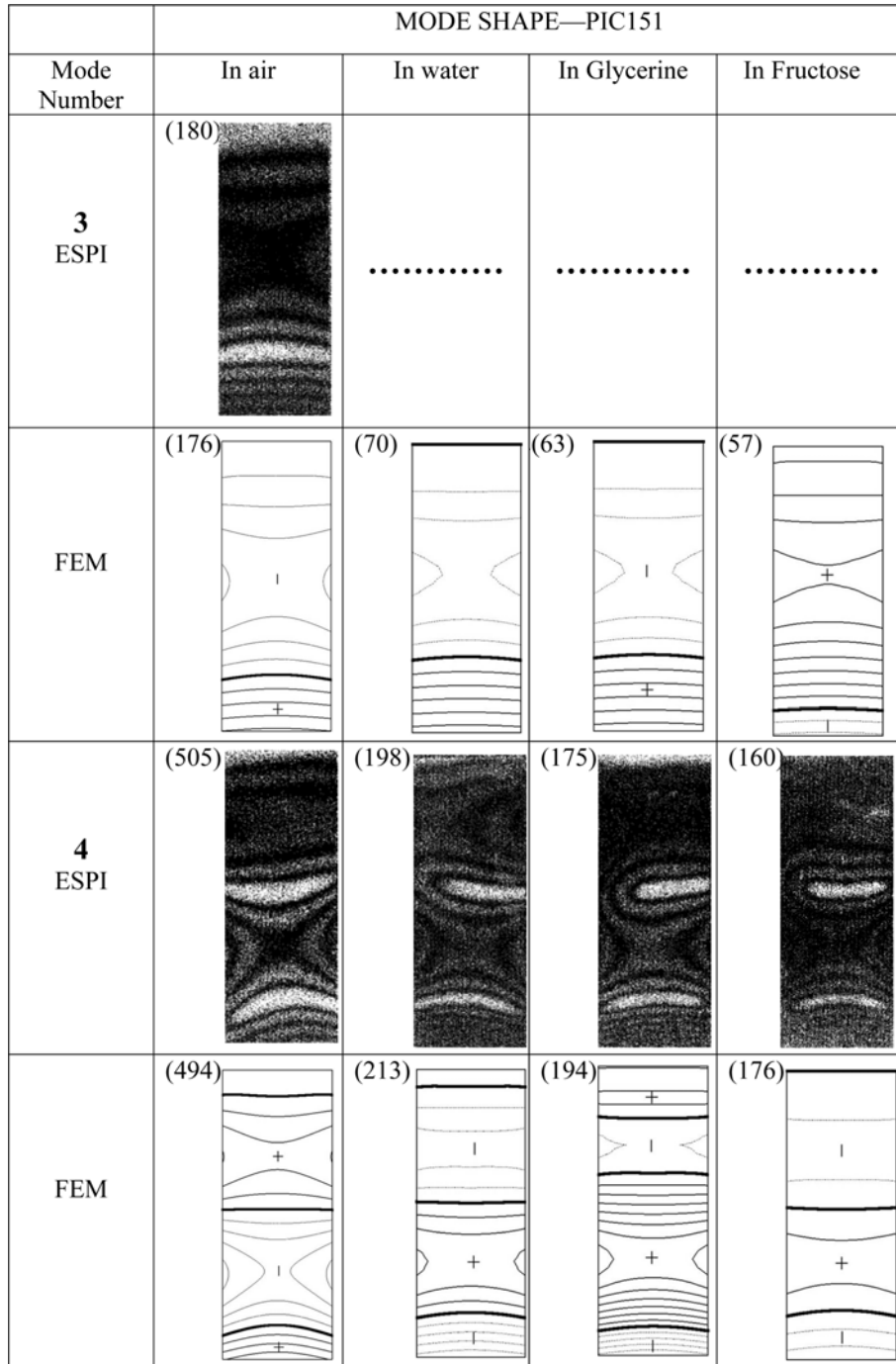


Fig. 3 continued

dynamic analysis. In the in-fluid analysis, the shell element is used to model the piezoceramic plate and the three-dimensional acoustic element is used to model the fluids.

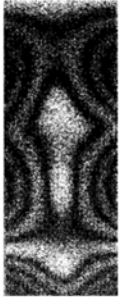
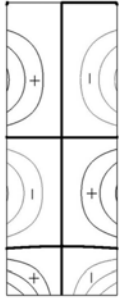
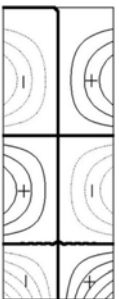
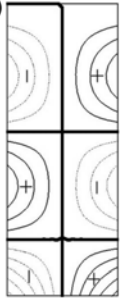
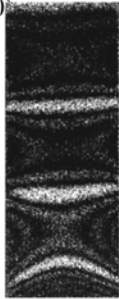
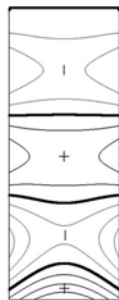
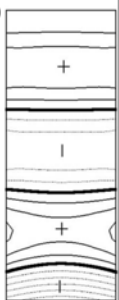
		MODE SHAPE—PIC151			
Mode Number	In air	In water	In Glycerine	In Fructose	
<b>5</b> ESPI	(870) 	.....	.....	.....	
	FEM (883) 	(478) 	(440) 	(404) 	
<b>6</b> ESPI	(1010) 	(440) 	(375) 	(355) 	
	FEM (971) 	(455) 	(415) 	(379) 	

Fig. 3 continued

The acoustic medium is used in the problem for the transmission of acoustic wave. It is elastic and only sustains the hydrostatic stress. The constitutive relation is  $\sigma = K_f \varepsilon_V$ , where  $\varepsilon_V$  is the

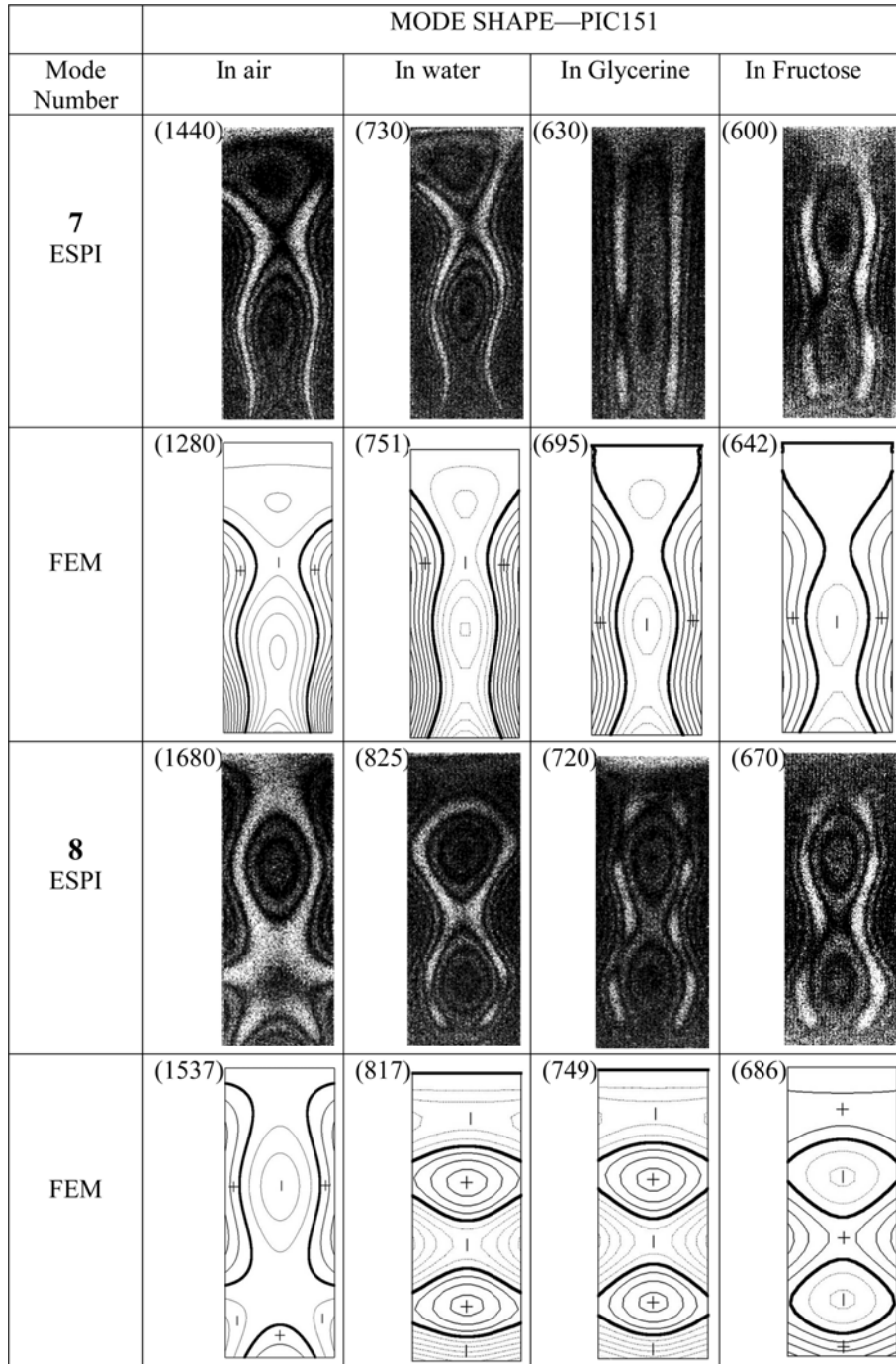


Fig. 3 continued

volumetric strain ( $\epsilon_V = \epsilon_{11} + \epsilon_{22} + \epsilon_{33}$ ), and  $K_f$  is the bulk modulus. The equilibrium equation for small motions of the compressible, adiabatic fluid is taken to be

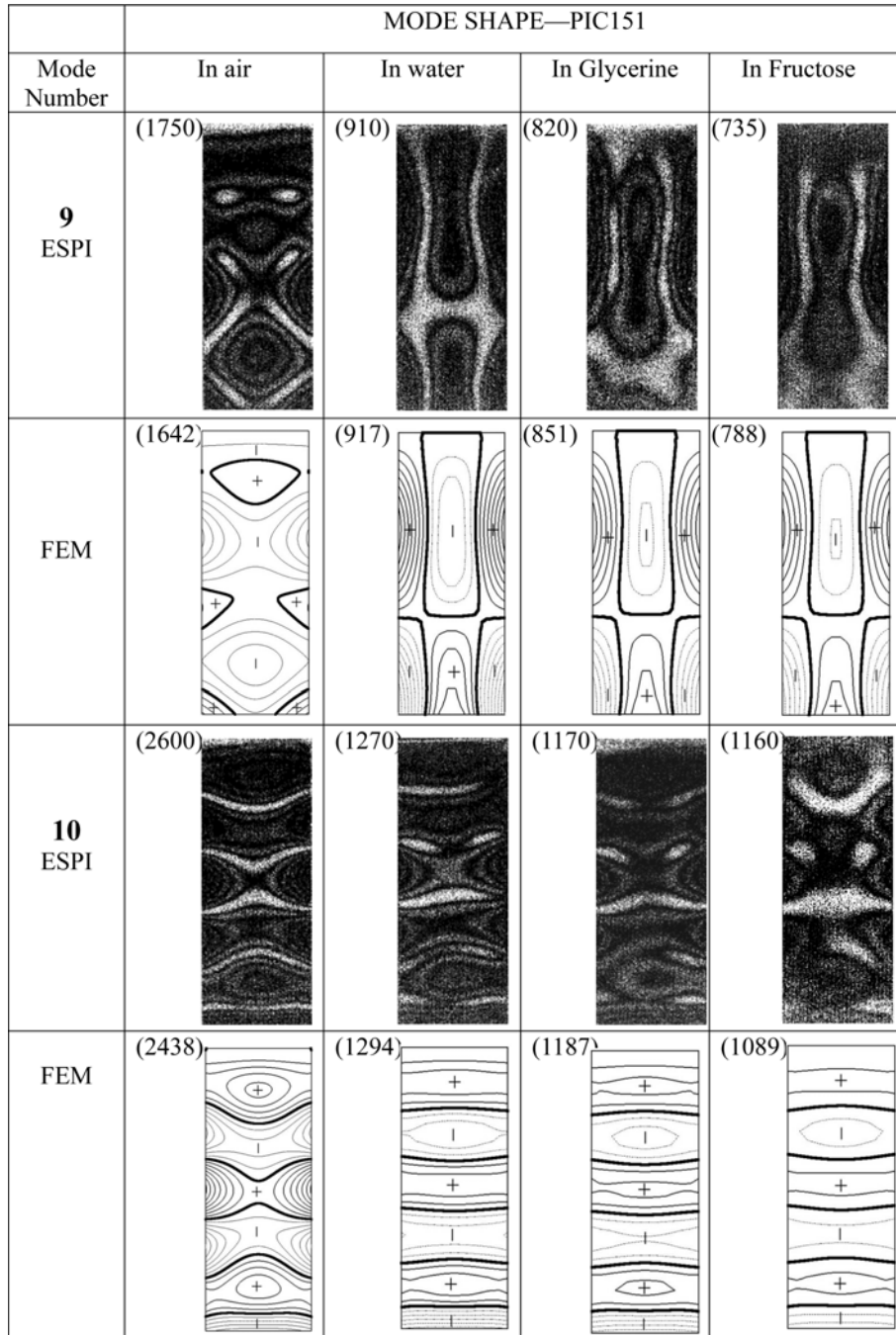


Fig. 3 continued

$$\frac{\partial p}{\partial x} + \gamma \dot{u}^f + \rho_f \ddot{u}^f = 0 \tag{6}$$

Table 3 Resonant frequencies of cantilevered piezoceramic plates in air and fluid measured from AF-ESPI experiments and FEM computations

PIC151		Resonant Frequency (Hz)			
Mode Number	Air		Water	Glycerine	Fructose
	Shell Model	Acoustic Analysis			
<b>1</b>		30	10	8	7
ESPI					
FEM	28	28	10	9	9
(Err%)	(-6.7)	(-6.7)	(0.0)	(12.5)	(28.6)
<b>2</b>		142	.....	.....	.....
ESPI					
FEM	150	150	77	71	65
(Err%)	(5.6)	(5.6)			
<b>3</b>		180	.....	.....	.....
ESPI					
FEM	176	176	70	63	57
(Err%)	(-2.2)	(-2.2)			
<b>4</b>		505	198	175	160
ESPI					
FEM	494	496	213	194	176
(Err%)	(-2.2)	(-1.8)	(7.6)	(10.9)	(10.0)
<b>5</b>		870	.....	.....	.....
ESPI					
FEM	883	886	478	441	404
(Err%)	(1.5)	(1.8)			
<b>6</b>		1010	440	375	355
ESPI					
FEM	971	980	455	415	379
(Err%)	(-3.9)	(-3.0)	(3.4)	(10.7)	(6.8)
<b>7</b>		1440	730	630	600
ESPI					
FEM	1280	1286	751	695	642
(Err%)	(-11.1)	(-10.7)	(2.9)	(10.3)	(7.0)
<b>8</b>		1680	825	720	670
ESPI					
FEM	1537	1544	817	749	686
(Err%)	(-8.5)	(-8.1)	(-1.0)	(4.0)	(2.4)
<b>9</b>		1750	910	820	735
ESPI					
FEM	1642	1670	917	851	788
(Err%)	(-6.2)	(-4.6)	(0.8)	(3.8)	(7.2)
<b>10</b>		2600	1270	1170	1160
ESPI					
FEM	2438	2607	1294	1187	1089
(Err%)	(-6.2)	(0.3)	(1.9)	(1.5)	(-6.1)

where  $p$  is the pressure in the fluid,  $x$  is the spatial position of the fluid particle,  $\dot{u}^f$  is the fluid particle velocity,  $\ddot{u}^f$  is the fluid particle acceleration,  $\rho_f$  is the density of the fluid, and  $\gamma$  is the volumetric drag. When the acoustic medium is adjacent to the structure, the acoustic-structural coupling effect should be considered. The displacement, acoustic pressure, temperature, and electrical potential of the nodes of the fluid on the interface have the same value as the nearest nodes of the structure on the interface. The pressure on the upper free surface of the fluid is set to be zero, and all the other surfaces of the vessel are set to be rigid. The piezoceramic plate is fixed in one side. To verify the model, we also apply this acoustic model to the in-air case, in which the fluid is changed to air.

The resonant frequencies measured from AF-ESPI and calculated from FEM analysis are listed in Table 3. The resonant frequencies and correspondent mode shapes for the first ten modes of the cantilevered piezoceramic plate obtained from experimental measurement and FEM computation are listed in Fig. 3 for comparison. From the experimental and FEM results shown in Table 3 and Fig. 3, we find that the resonant frequencies of the cantilevered piezoceramic plate in fluid are much lower than those in air. The resonant frequencies decrease with the increase in the density and the viscosity of the fluid. From Table 3, it is shown that the numerical results of the resonant frequencies are consistent with the experimental ones. The FEM results agree with the AF-ESPI experimental ones very well in the in-fluid model and the error is less than 11%. The error may be caused from the numerical computation, the imperfection of the boundary conditions in the experimental measurement, and uncertainty of the material constants of piezoceramic material. Hence it is noted that the shell element, which neglects the piezoelectric effect, can be used to predict the vibration characteristics of the piezoceramic plate in fluid.

In order to verify the in-fluid FEM model, we also consider the air as a fluid and compare the numerical result with the in-air model that neglects the effect of air. These results are also shown in Table 3. We can see that the results are similar for both models while the resonant frequencies predicted from the acoustic model are slightly larger than the in-air model.

It is evident from Fig. 3 that the mode shapes of the cantilevered piezoceramic plate obtained from both AS-ESPI experimental measurement and FEM analysis are similar in air and fluids. The second, third, and fifth modes can not be easily excited in fluid. Furthermore, the sequence of the eighth and ninth modes is changed and the correspondent mode shapes of in-air and in-fluid are quite different. We also find that with the increase in the density and viscosity of the fluids, i.e., the glycerine and the fructose, the displacements decrease. Generally speaking, due to the disturbance of the fluid in the experimental measurement, the fringe pattern obtained is not as clear as that in air, especially for the higher modes.

## 5. Conclusions

The ultrasound transducers are widely used as acoustic sources in fluid such as sea water or petroleum. Since the piezoelectric materials can collect the electrical and the mechanical energies, they are commonly used in ultrasound transducers. It is important for us to analyze the vibration characteristics of piezoceramic plates in fluid because of their particular applications. In this study, the out-of-plane vibration characteristics of a cantilevered piezoceramic plate in air and in fluid are investigated in detail by theoretical calculations and experimental measurements. A full-field optical method based on the amplitude fluctuation ESPI (AF-ESPI) technique with good fringe visibility

and noise reduction has been used to obtain the resonant frequencies and corresponding mode shapes of the cantilevered piezoceramic plate. The resonant frequencies and mode shapes of the cantilevered piezoceramic plate are also presented by FEM to compare with the results obtained by AF-ESPI. From the results presented in this paper, it is noted that the acoustic FEM model can be used to determine the resonant frequencies and mode shapes of piezoceramic plates in fluid. The quality of the fringe pattern in the AF-ESPI experiment for the cantilevered piezoceramic plate in air is generally good. However, the difficulty to obtain good quality of fringe pattern increase as the density and the viscosity of the fluid increase. The full-field mode shapes in resonance obtained by using the AF-ESPI method, together with the theoretical results of finite element calculation provide complete information for the vibration characteristics of the piezoceramic plate in fluid.

### Acknowledgements

The authors gratefully acknowledge the financial support of this research by National Science Council (Republic of China) under Grant NSC94-2212-E002-018.

### References

- Balabaev, S.M. and Ivina, N.F. (2001), "Acoustic radiation of a water-filled piezoelectric cylinder near a rigid plane", *Acoustical Physics*, **47**(3), 247-252.
- Butters, J.N. and Leendertz, J.A. (1971), "Speckle patterns and holographic techniques in engineering metrology", *Optics and Laser Technology*, **3**(1), 26-30.
- Ekeom, D., Dubus, B. and Granger, C. (1998), "Coupled finite-element wave number decomposition method for the modeling of piezoelectric transducers radiating in fluid-filled boreholes", *J. Acoust. Soc. Am.*, **104**(5), 2779-2789.
- Graham, G., Petzing, J., Lucas, M., and Tyrer, J. (1999), "Quantitative modal analysis using electronic speckle pattern interferometry", *Optics Lasers Eng.*, **37**(2), 147-161.
- Huang, C.H. and Ma, C.C. (1998), "Vibration characteristics for piezoelectric cylinders using amplitude-fluctuation electronic speckle pattern interferometry", *AIAA J.*, **36**(12), 2262-2268.
- Jones, R. and Wykes, C. (1989), *Holographic and Speckle Interferometry*, Cambridge Univ. Press, England.
- Ma, C.C. and Huang, C.H. (2001), "The investigation of three-dimensional vibration for piezoelectric rectangular parallel pipes using the AF-ESPI method", *IEEE Transactions on Ultrasonics, Ferroelectrics and Frequency Control*, **48**(1), 142-153.
- Nakadate, S., Saito, H. and Nakajima, T. (1986), "Vibration measurement using phase-shifting stroboscopic holographic interferometry", *Optical Acta.*, **33**(10), 1295-1309.
- Oswin, J.R., Salter, P.L., Santoyo, F.M., and Tyrer, J.R. (1994), "Electronic speckle pattern interferometric measurement of flextensional transducer vibration patterns: in air and water", *J Sound Vib.*, **172**(4), 433-448.
- Petzing, J.N., Tyrer, J.R. and Oswin, J.R. (1996), "Improved interferometric techniques for measuring flextensional transducer vibration patterns underwater", *J. Sound Vib.*, **193**(4), 877-890.
- Savin, E. (2008), "A transport model for high-frequency vibrational power flows in coupled heterogeneous structures", *Interaction and Multiscale Mechanics, An Int. J.*, **1**(1), 53-81.
- Shellabear, M.C. and Tyrer, J.R. (1991), "Application of ESPI to three-dimensional vibration measurements", *Optics Lasers Eng.*, **15**, 43-56.
- Wang, W.C., Hwang, C.H., and Lin, S.Y. (1996), "Vibration measurement by the time-averaging electronic speckle pattern interferometry method", *Applied Optics*, **35**(22), 4502-4509.